

## Viscosity and structure configuration properties of equilibrium and supercooled liquid cobalt

R. M. Khusnutdinoff, A. V. Mokshin, A. L. Beltyukov & N. V. Olyanina

To cite this article: R. M. Khusnutdinoff, A. V. Mokshin, A. L. Beltyukov & N. V. Olyanina (2018): Viscosity and structure configuration properties of equilibrium and supercooled liquid cobalt, *Physics and Chemistry of Liquids*, DOI: [10.1080/00319104.2018.1461871](https://doi.org/10.1080/00319104.2018.1461871)

To link to this article: <https://doi.org/10.1080/00319104.2018.1461871>



Published online: 16 Apr 2018.



Submit your article to this journal [↗](#)



View related articles [↗](#)



View Crossmark data [↗](#)

ARTICLE



# Viscosity and structure configuration properties of equilibrium and supercooled liquid cobalt

R. M. Khusnutdinoff<sup>a</sup>, A. V. Mokshin<sup>a</sup>, A. L. Beltyukov<sup>b</sup> and N. V. Olyanina<sup>b</sup>

<sup>a</sup>Department of Computational Physics, Institute of Physics, Kazan (Volga region) Federal University, Kazan, Russia; <sup>b</sup>Udmurt Federal Research Center of the Ural Branch of the Russian Academy of Sciences, Izhevsk, Russia

## ABSTRACT

The shear viscosity of liquid cobalt at the pressure  $p = 1.5$  bar and at the temperatures corresponding to equilibrium liquid and supercooled liquid states is measured experimentally and evaluated by means of molecular dynamics simulations. Further, the shear viscosity is also calculated within the microscopic theoretical model. Comparison of our experimental, simulation and theoretical results with other available data allows one to examine the issue about the correct temperature dependence of the shear viscosity of liquid cobalt. A strong correlation between the viscosity and the configuration entropy of liquid cobalt over the considered temperature range is found, which can be taken into account by the Rosenfeld's model.

## ARTICLE HISTORY

Received 1 February 2018

Accepted 3 April 2018

## KEYWORDS

Liquid cobalt; molecular dynamics; entropy; viscosity; scaling law

## Introduction

Cobalt is inferior to iron, aluminium and copper in the degree of use in the ordinary metallurgical industry. Nevertheless, due to its physical properties, cobalt is applied in the aerospace industry. In particular, cobalt-based alloys stand out by the following properties such as high strength, corrosion resistance and hardness extended over a wide temperature range. Similar to a simple single-component system, pure cobalt is not inclined to generate an amorphous phases. Cobalt melt crystallises at low and moderate levels of the supercooling, and at values of the viscosity  $\eta$  much smaller than  $\eta \simeq 10^{12}$  Pa·s. Thus, the deep supercooling levels with the temperatures lower than the glass transition temperature  $T_g$  are not attainable for the case of cobalt. Nevertheless, as follows from recent results [1,2], the inclusion of cobalt in the composition of metallic melts can enhance their glass-forming abilities.

The viscosity is one of the main characteristic of a system, which defines its crystallisation and glass-forming ability [3–5]. In particular, the viscosity determines directly the crystal nucleation and growth rates, as well as the ability to generate and to retain a disordered state [6]. For the case of liquid cobalt, there is an ambiguous situation with regard to temperature dependence of the viscosity  $\eta(T)$ . The known experimental data for the viscosity  $\eta(T)$  of liquid cobalt [7–9] has a difference in values about 30% and even more. To our knowledge, there are no experimental data on the viscosity of supercooled cobalt. Therefore, one of the purposes of the given study is to refine values of the shear viscosity of cobalt for the equilibrium liquid phase (at the temperatures higher the melting temperature  $T_m = 1768$  K, where  $\eta(T_m) = 5.4$  mPa·s [7]) and to evaluate the viscosity of the supercooling liquid cobalt (with the temperatures  $T < T_m$ ). Thus, we present experimental and molecular dynamics simulation results of the shear viscosity of liquid cobalt for the temperature range  $T = [1400; 2000]$  K and at the pressure  $p = 1.5$  bar. Furthermore, the

temperature dependence  $\eta(T)$  is also calculated within the microscopic theoretical model where the parameters are computed on the basis of the configuration data of the system.

As follows from statistical mechanics [10,11], the viscosity of a (dense, condensed) system is defined by the interparticle interaction energy and by the structural characteristics. This is clearly seen from the microscopic expressions for the viscosity suggested by Born and Green [12] and by Irving and Kirkwood [13] and applied usually to compute the viscosity on the basis of molecular dynamics simulation data. Further, pronounced correlation effects between the viscosity and the configuration entropy, which are accounted for by the Rosenfeld's and Dzugutov's relations, were established for various metallic melts [14–21] and a lot of molecular liquids under high pressure [22–26]. Therefore, the correlation between the viscosity and the structure configuration properties of liquid cobalt over the considered temperature range is also verified in the given study.

## Experimental details

The viscosity of liquid cobalt for the temperatures over the range from  $T = 1506$  to  $1969$  K has been experimentally measured by the method of torsional vibrations of a cylindrical crucible with the melt [27,28]. The mass fraction of cobalt in the samples was no less than 99.98%, while the samples could also contain the following impurities: less than 0.003% of Fe, less than 0.005% of Ni and C, less than 0.001% of Si, Cu, Mg, Zn and Al, and less than 0.001% of O. The cylindrical crucibles with the internal diameter  $\sim 17$  mm and height  $\sim 42$  mm were made from  $\text{Al}_2\text{O}_3$ . The temperature dependence of the viscosity was measured by heating of the samples from the melting temperature  $T_m$  up to the temperature  $T = 1973$  K. Then, the samples were cooled until they crystallised. The temperature step of the heating/cooling procedure was  $\Delta T = 20 \pm 5$  K, and the melt samples were equilibrated at each temperature over 20 min. Experimental value of the temperature was determined with the precision  $\pm 5$  K by means of the tungsten–rhenium thermocouple calibrated for the melting points of pure Al, Cu, Ni and Fe.

The kinematic viscosity  $\nu$  was evaluated by means of numerical solution of the motion equation of the cylindrical crucible [27,28]:

$$\text{Re}[L(\nu)] + \frac{\delta}{2\pi} \text{Im}[L(\nu)] - 2I \left( \frac{\delta}{\tau} - \frac{\delta_0}{\tau_0} \right) = 0. \quad (1)$$

where  $I$  is the moment of inertia;  $\delta$  and  $\tau$  are the attenuation decrement and the oscillation period of the system with the melt, whereas  $\delta_0$  and  $\tau_0$  are the same characteristics for the empty crucible, respectively. Finally,  $\text{Re}[L]$  and  $\text{Im}[L]$  are the real and imaginary parts of the friction function  $L$ , which is related to the kinematic viscosity  $\nu$  (see [27], for details).

The average linear coefficient of the thermal expansion for the crucible material  $\text{Al}_2\text{O}_3$  over the temperature range from 273 K to 2073 K takes the value  $9.0 \cdot 10^{-6} \text{ deg}^{-1}$  ([29].), and the possible impact of the thermal expansion on the measured values of the viscosity must be also taken into account. The height of the melt within the crucible is determined as

$$H = \frac{M}{\pi R^2 \rho_\mu}. \quad (2)$$

Here,  $M$  is the mass of the sample and  $\rho_\mu$  is the mass density of the melt, which was defined from the relation

$$\rho_\mu(T) = 6172.152 - 0.936T. \quad (3)$$

suggested in [8].

## Details of simulation and numerical calculation

Molecular dynamic simulations of liquid cobalt were carried out for the isothermal–isobaric (NpT) ensemble for the temperatures from the range  $T = [1400; 2000]$  K and at the pressure  $p = 1.5$  bar. The system consisted of  $N = 4000$  atoms located in a cubic cell with periodic boundary conditions. Interaction between atoms was carried out using the Embedded Atom Method (EAM) potential [30,31]. The equations of motion for atoms were integrated using the velocity Verlet algorithm with the time step  $\tau = 1.0$  fs [32]. To bring the system into a state of thermodynamic equilibrium and to calculate the temporal and spectral characteristics of the system, the dynamics with 100,000 and 2000,000 time steps, respectively, was realised.

The shear viscosity can be determined in the framework of the Green–Kubo approach [33] through the autocorrelation functions of the stress tensor,  $\sigma_{\alpha,\beta}$ . The non-diagonal components of the stress tensor are given by [34]

$$\sigma_{\alpha,\beta} = \frac{1}{V} \left( \sum_{i=1}^N m v_{i\alpha} v_{i\beta} - \sum_{i=1}^{N-1} \sum_{j=i+1}^N r_{ij\alpha} \frac{\partial U(r_{ij})}{\partial r_{ij\beta}} \right), \quad (4)$$

where  $\vec{r}_i$ ,  $\vec{v}_i$  are the position and the velocity of a particle;  $i, j$  are the numbers of particles;  $\vec{r}_{ij} = \vec{r}_i - \vec{r}_j$ ,  $U(r_{ij})$  is the particle interaction potential;  $\alpha, \beta$  are the indices of the components of the corresponding vectors;  $m$  is the particle mass and  $V$  is the volume of the system. Then, the shear viscosity can be calculated by the formula:

$$\eta = \frac{V}{k_B T} \int_0^\infty \langle \sigma_{\alpha,\beta}(t) \sigma_{\alpha,\beta}(0) \rangle dt, \quad (5)$$

where  $k_B$  is the Boltzmann constant.

## Theoretical formalism

Let us consider a system consisting of  $N$  identical particles of mass  $m$  enclosed in the volume  $V$ . We take the off-diagonal component of the stress tensor  $\sigma_{\alpha,\beta}$ , defined by Equation (4), as the initial dynamic variable. Then, we determine the time correlation function (TCF) of the stress tensor as follows [35]:

$$S(t) = \frac{\langle \sigma_{\alpha,\beta}(t) \sigma_{\alpha,\beta}(0) \rangle}{\langle |\sigma_{\alpha,\beta}(0)|^2 \rangle}, \quad (6)$$

and its spectral density as the next [36]:

$$\tilde{S}(\omega) = \frac{S_0}{2\pi} \text{Re} \int_{-\infty}^{\infty} e^{i\omega t} S(t) dt. \quad (7)$$

Here,  $S_0$  is the zeroth frequency moment of  $\tilde{S}(\omega)$  ([37]):

$$S_0 = \langle |\sigma_{\alpha,\beta}(0)|^2 \rangle = \left( \frac{k_B T}{V} \right)^2 + \frac{2\pi\rho k_B T}{15 V^2} \int_0^\infty r^4 g(r) \left( \frac{4}{r} \frac{\partial \mathcal{U}}{\partial r} + \frac{\partial^2 \mathcal{U}}{\partial r^2} \right) dr, \quad (8)$$

$\rho$  is the number density, and  $g(r)$  is the pair radial distribution function.

On the other hand, according to the formalism of the TCFs [33,38], the spectral density of TCF of the stress tensor  $\tilde{S}(\omega)$  can be represented as infinite continuous fraction:

$$\tilde{S}(\omega) = \frac{1}{\pi} \operatorname{Re} \left\{ \frac{S_0}{i\omega + \frac{\Delta_1}{i\omega + \frac{\Delta_2}{\dots}}} \right\}. \quad (9)$$

Here,  $\Delta_n$ ,  $n = 1, 2, 3, \dots$  are the relaxation parameters, which are related with the frequency moments  $S^{(2m)}$  of  $\tilde{S}(\omega)$ :

$$S^{(2j)} = \frac{\int \omega^{2j} \tilde{S}(\omega) d\omega}{\int \tilde{S}(\omega) d\omega}, \quad j = 1, 2, \dots \quad (10)$$

by means of the following expressions:

$$\begin{aligned} \Delta_1 &= S^{(2)}, \\ \Delta_2 &= \frac{S^{(4)}}{S^{(2)}} - S^{(2)}, \\ \Delta_3 &= \frac{S^{(6)}S^{(2)} - S^{(4)^2}}{S^{(4)}S^{(2)} - S^{(2)^3}, \dots \end{aligned}$$

The relaxation parameters can be determined numerically from molecular dynamic simulation data in accordance with the basic definitions [39]:

$$\Delta_n = \frac{\langle |A_n(0)|^2 \rangle}{\langle |A_{n-1}(0)|^2 \rangle}, \quad n = 1, 2, \dots, \quad (11)$$

where

$$\begin{aligned} A_0(t) &= \sigma_{\alpha\beta}(t), \\ A_1(t) &= \frac{\partial A_0(t)}{\partial t}, \\ A_2(t) &= \frac{\partial A_1(t)}{\partial t} + \Delta_1 A_0(t), \\ &\dots, \\ A_n(t) &= \frac{\partial A_{n-1}(t)}{\partial t} + \Delta_{n-1} A_{n-2}(t). \end{aligned} \quad (12)$$

As shown in [40,41], alignment of the relaxation scales  $\Delta_2^{-1/2} \approx \Delta_3^{-1/2} \approx \Delta_4^{-1/2}$  is observed for the transport processes in monatomic liquids. This allows one to obtain expression for the spectral density  $\tilde{S}(\omega)$ :

$$\tilde{S}(\omega) = \frac{1}{\pi} \frac{2\Delta_1 \Delta_2 \sqrt{4\Delta_2 - \omega^2}}{\Delta_1^2 (4\Delta_2 - \omega^2) + \omega^2 (2\Delta_2 - \Delta_1)^2}. \quad (13)$$

Then, in accordance with the Green–Kubo formula (5), and we obtain the following expression for the shear viscosity:

$$\eta = \frac{VS_0}{\pi k_B T} \frac{\sqrt{\Delta_2}}{\Delta_1}. \quad (14)$$

Taking into account Equation (8) for  $S_0$  and neglecting the kinetic contribution, one can see that Equation (14) transforms into the Rice–Kirkwood approximated equation for the viscosity at the melting temperature [42]:

$$\eta = \frac{2\pi m \rho^2}{15\zeta_f} \int_0^\infty r^4 \left( \frac{4}{r} \frac{\partial \mathcal{U}}{\partial r} + \frac{\partial^2 \mathcal{U}}{\partial r^2} \right) g(r) dr, \quad (15)$$

where the friction coefficient  $\zeta_f$  is equal to

$$\zeta_f = \frac{\pi m \rho V \Delta_1}{\sqrt{\Delta_2}}. \quad (16)$$

On the other hand, using the expression for the viscosity (7.32) from [43].

$$\eta \approx 4.38 \omega_0 m \rho^2 g(r_m) r_m^5 (1 - r_0/r_m) \quad (17)$$

and the viscosity values obtained from formula (14), one can estimate the characteristic frequency of atomic vibration  $\omega_0$ :

$$\omega_0 = \frac{V S_0 \sqrt{\Delta_2}}{4.38 \pi k_B T \Delta_1 m \rho^2 g(r_m) r_m^5 (1 - r_0/r_m)}. \quad (18)$$

Here,  $r_0$  is the minimum possible distance between neighbouring atoms [where  $g(r)$  starts to take non-zero values],  $r_m$  is location of the main maximum of  $g(r)$ .

## Results

In Figure 1, the spectral density  $\tilde{S}(\omega)$  of liquid cobalt obtained from molecular dynamic simulations results is presented and compared with theoretical results [Equation (13)] at various temperatures. The relaxation parameters  $\Delta_1$  and  $\Delta_2$  were determined numerically from Equations (11) and (12). As seen from Figure 1, theoretical curves reproduce correctly the spectra  $\tilde{S}(\omega)$  for the considered temperature range.

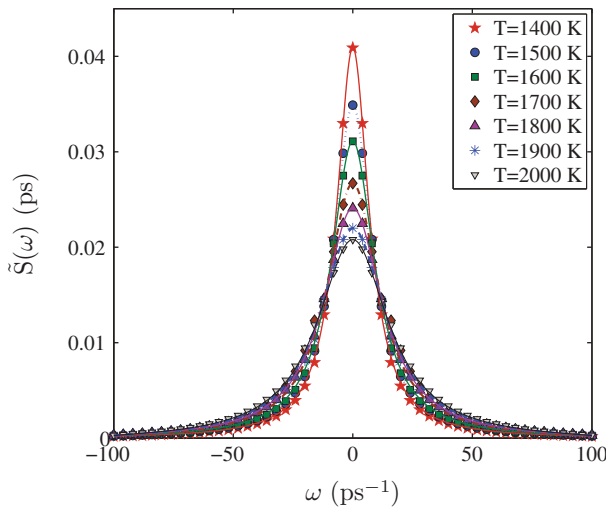


**Figure 1.** (Color online) Spectral density of the stress tensor TCF of cobalt melt at different temperatures: markers represent simulation data; lines – the results of theoretical calculations with the expression (13).

Figure 2 shows the shear viscosity of liquid cobalt as a function of the inverse temperature in logarithmic scale. The plot is constructed on the basis of the experimental data, the simulation results and the theoretical calculations with Equation (14). As seen from Figure 2, the experimental data, simulation and theoretical results are reproduced fairly well by the Arrhenius law [45]

$$\eta(T) = \eta_0 \exp(E/k_B T). \quad (19)$$

Here,  $\eta_0$  is the pre-exponential factor corresponding formally to the viscosity at  $T \rightarrow \infty$ ;  $E$  is the activation energy. For our simulation results and the experimental data, we find the parameters  $\eta_0^{MD} = 0.29 \text{ mPa} \cdot \text{s}$  ( $\eta_0^{Exp} = 0.34 \text{ mPa} \cdot \text{s}$ ) and  $E^{MD} = 6.6 \cdot 10^{-20} \text{ J}$  ( $E^{Exp} = 6.5 \cdot 10^{-20} \text{ J}$ ), respectively.

Inset of Figure 2 represents the temperature dependence of the characteristic frequency  $\omega_0(T)$  of atomic vibrations found from Equation (18). As can be seen, for the temperature range  $T = [1800, 2000] \text{ K}$ , the dependence  $\omega_0(T)$  is well reproduced by the Arrhenius law with the pre-exponential factor  $\Omega_0 = 0.225 \text{ ps}^{-1}$  and the activation energy  $E = 6.6 \cdot 10^{-20} \text{ J}$ , which coincides completely with the activation energy of the viscous process. Deviation from the Arrhenius law in the temperature dependence  $\omega_0(T)$  below the melting temperature  $T_m$  is due to the fact that Equation (17) can be applied only to the equilibrium liquid.

Expression (14) for the shear viscosity  $\eta$  contains the frequency parameters  $\Delta_1$  and  $\Delta_2$ , which are determined through the configuration characteristics of the system, namely, through the two- and three-particle distribution functions [46]. Therefore, it is advisable to consider a possible correlation between the viscosity and structural characteristics of the system (e.g. configuration entropy [22–24]).

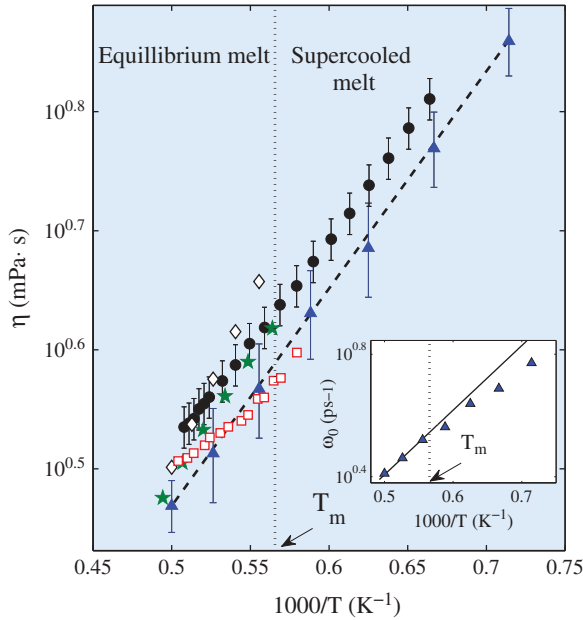


**Figure 2.** (Color online) Main: Temperature dependence of the shear viscosity for liquid cobalt at the pressure  $p = 1.5 \text{ bar}$ : markers ( $\Delta \Delta \Delta$ ) represents the results of the molecular dynamic simulations calculated by Green–Kubo relation for the TCF of the stress tensor  $S(t)$ ; ( $\circ \circ \circ$ ) – the experimental results; the dashed line represents the results of theoretical calculations performed according to the formula (14); markers ( $\diamond \diamond \diamond$ ), ( $***$ ) and ( $\square \square \square$ ) are the experimental data taken from [8,9] and [44], respectively. Inset: Time dependence of the characteristic frequency of atom vibration: markers ( $\Delta \Delta \Delta$ ) represent the molecular dynamic data; The solid line – the results of fitting by the Arrhenius law.

Probably, the most well-known expression, where such a relationship is assumed, is the Adam–Gibbs relation [47]:

$$\eta = A \exp(C/TS_C). \quad (20)$$

Here,  $S_C$  is the configuration entropy and  $C$  is the constant characterised by the barrier height of atomic restructuring. On the other hand, the Rosenfeld's scaling laws states the relation between the excess entropy  $S_{ex}$  and the transport coefficients such as the self-diffusion  $D$ , the viscosity  $\eta$  and the thermal conductivity  $\kappa$  of the system [48,49]:

$$D^* = D \frac{\rho^{1/3}}{(k_B T/m)^{1/2}} = A \exp(-\alpha S_{ex}), \quad (21a)$$

$$\eta^* = \eta \frac{\rho^{-2/3}}{(mk_B T)^{1/2}} = B \exp(\beta S_{ex}), \quad (22b)$$

$$\kappa^* = \kappa \frac{\rho^{-2/3}}{k_B(k_B T/m)^{1/2}} = C \exp(\gamma S_{ex}). \quad (23c)$$

Here,  $A$ ,  $B$ ,  $C$ ,  $\alpha$ ,  $\beta$  and  $\gamma$  are the property-specific constants which are equal for model fluids to 0.6, 0.2, 1.5, 0.8, 0.8 and 0.5, respectively [49]. The quantities  $D^*$ ,  $\eta^*$  and  $\kappa^*$  are dimensionless, the excess entropy  $S_{ex}$  is given in units of  $k_B$ . The Rosenfeld's scaling relation (21b) for the viscosity may be considered as an attempt to realise the following physical idea. Since the viscosity is simply proportional to the structural relaxation time, then according to relation (21b), the viscosity is proportional to the number of accessible configurations with the structural relaxation time [24–26].

The thermodynamic excess entropy is defined as the difference in entropy between the fluid and the corresponding ideal gas under identical temperature and density conditions. The total entropy of a classical fluid can be written as [50]

$$S = S_{id} + \sum_{n=2}^N S_n, \quad (22)$$

where  $S_{id}$  is the entropy of the ideal gas reference state and  $S_n$  is the entropy contribution due to  $n$ -particle spatial correlations. Then, the excess entropy is defined as

$$S_{ex} = S - S_{id}. \quad (23)$$

The main contribution into  $S_{ex}$  is due to the pair-correlation entropy  $S_2$  which is  $\sim 85 \div 95\%$  for the case of monatomic liquids over a fairly wide range of densities. Therefore, the next approximation can be applied:  $S_{ex} \approx S_2$ . The pair-correlation entropy is defined as

$$\begin{aligned} S_2 = & -2\pi\rho \int_0^\infty \{g(r) \ln(g(r)) - [g(r) - 1]\} r^2 dr = \\ & -2\pi\rho \int_0^\infty g(r) \ln(g(r)) r^2 dr + \frac{1}{2} (\rho k_B T \chi_T - 1), \end{aligned} \quad (24)$$

where  $\chi_T$  is the isothermal compressibility.

In Figure 3, the reduced shear viscosity in logarithmic scale is shown at the corresponding values of the negative excess entropy  $S_{ex}$  [using two-particle approximation (24)]. First, our experimental values and experimental data from [8,9] as well as MD simulation results and theoretical results from Equation (14) yield the straight lines that are in agreement with the Rosenfeld's scaling representation (21b). Further,  $\eta^*(S_{ex})$  dependence with experimental data from



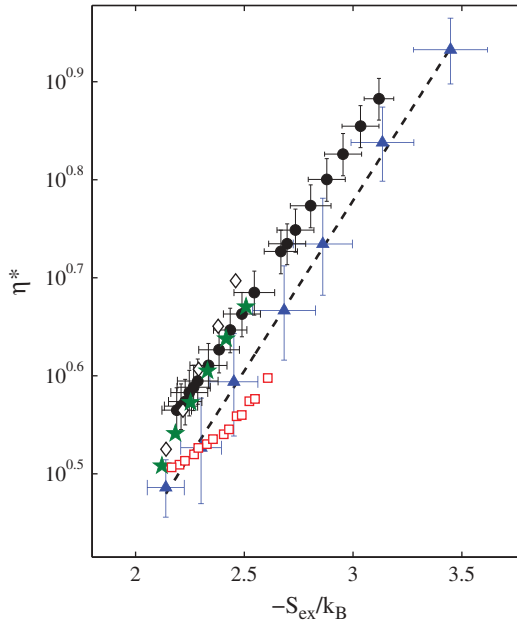


**Figure 3.** (Color online) Rosenfeld’s scaling law for the reduced shear viscosity  $\eta^*$  with the pair-excess entropy  $S_{ex}$  for liquid cobalt at the pressure  $p = 1.5$  bar: markers ( $\Delta\Delta\Delta$ ) represent the results of molecular dynamic simulations calculated using the Green–Kubo relation for the TCF of the stress tensor  $S(t)$ ; ( $\circ\circ\circ$ ) – the experimental results; solid line represents the results of the calculations performed according to the formula (14); markers ( $\diamond\diamond\diamond$ ), ( $\star\star\star$ ) and ( $\square\square\square$ ) are the experimental data taken from [8,9] and [44], respectively.

[8,9] differs from these lines. Second, the Rosenfeld’s scaling extends well to the temperature range of the supercooling melt, which is verified by the scaled representation of our experimental data as well as of our simulation and theoretical results. Third, our experimental data, simulation data and theoretical results for the shear viscosity yield the same slope in the Rosenfeld’s scaling plot with the parameter  $\beta_{exp} = 0.78 \pm 0.02$  [see Equation (21b)]. Note that this value is close to  $\beta \approx 0.8$ , which is usually expected for the monoatomic fluids [49]. The prefactor  $B$  is estimated to be 0.68 and 0.6 for our experimental data and theoretical (simulation) results for the viscosity, respectively; and  $B = 0.27$  for the data from [8].

## Conclusions

In summary, the shear viscosity of liquid cobalt at different temperatures was determined experimentally and numerically by means of molecular dynamic simulations with the EAM interparticle interaction potential [30]. Further, the spectral densities of the stress tensor TCF  $\tilde{S}(\omega)$  as well as the shear viscosity  $\eta$  are computed within the framework of the microscopic theoretical model [40,41]. A good agreement between theoretical results, experimental data and molecular dynamic simulation results for the viscosity of liquid cobalt was found. It is shown that experimental data as well as simulation and theoretical results for the shear viscosity are reproduced by the Rosenfeld’s model.

## Acknowledgements

This work related with simulations supported in part by the Russian Foundation for Basic Research (project No. 18-02-00407-a). The authors are also grateful to the Ministry of Education and Science of the Russian Federation for supporting the research in the framework of the state assignment (No. 3.2166.2017/4.6).

## Disclosure statement

No potential conflict of interest was reported by the authors.

## Funding

This work was supported by the Russian Foundation for Basic Research [project No. 18-02-00407-a]. Authors are also grateful to the Ministry of Education and Science of the Russian Federation for supporting the research in the framework of the state assignment [No. 3.2166.2017/4.6].

## References

- [1] Luborsky FE, edited by. Amorphous metallic alloys. London: Butterworths; 1983.
- [2] Russev K, Stojanova L. Glassy metals. Berlin Heidelberg: Springer-Verlag; 2016.
- [3] Gaskell T, Balucani U, Vallauri R. Atomic transport in liquids. *Phys Chem Liq.* 1989;19:192–239.
- [4] Khusnutdinoff RM. Dynamics of a network of hydrogen bonds upon water electrocrystallization. *Colloid J.* 2013;75:726–732.
- [5] Khusnutdinoff RM. Structural and dynamic features of water and amorphous ice. *Colloid J.* 2017;79:152–159.
- [6] Fokin VM, Zanutto ED, Yuritsyn NS, et al. Homogeneous crystal nucleation in silicate glasses: a 40 years perspective. *J Non-Cryst Solids.* 2006;352:2681–2714.
- [7] Iida T, Guthrie RIL. The physical properties of liquid metals. Oxford: Oxford Press; 1988.
- [8] Assael MJ, Armyra IJ, Brillo J, et al. Reference data for the density and viscosity of liquid cadmium, cobalt, gallium, indium, mercury, silicon, thallium, and zinc. *J Phys Chem Ref Data.* 2012;41:033101(1)–033101(16).
- [9] CRC. Handbook of chemistry and physics, ed. by Lide DR. Boca Raton (FL): CRC Press; 2008.
- [10] Pitaevskii LP, Lifshitz EM. Statistical physics, Part 2: theory of the condensed state. Vol. 9. 1st ed. Oxford: Butterworth-Heinemann; 1980.
- [11] Evans DJ, Morris GP. Statistical mechanics of nonequilibrium liquids. London: Academic Press; 1990.
- [12] Born M, Green HS. A general kinetic theory of liquids. III. Dynamical properties. *Proc R Soc Lond A.* 1947;190:455–474.
- [13] Irving JH, Kirkwood JG. The statistical mechanical theory of transport processes. IV. The equations of hydrodynamics. *J Chem Phys.* 1950;18:817–829.
- [14] Dzugutov M. A universal scaling law for atomic diffusion in condensed matter. *Nature.* 1996;381:137–139.
- [15] Li GX, Liu CS, Zhu ZG. Scaling law for diffusion coefficients in simple melts. *Phys Rev B.* 2005;71:094209(1)–094209(7).
- [16] Samanta A, Ali SM, Ghosh SK. Universal scaling laws of diffusion: application to liquid metals. *J Chem Phys.* 2005;123:084505(1)–084505(5).
- [17] Ali SM. Scaling law of shear viscosity in atomic liquid and liquid mixtures. *J Chem Phys.* 2006;124:144504(1)–144504(8).
- [18] Fomin YD, Brazhkin VV, Ryzhov VN. Transport coefficients of soft sphere fluid at high densities. *JETP Lett.* 2012;95:320–325.
- [19] Gosh RC, Syed IM, Amin Z, et al. A comparative study on temperature dependent diffusion coefficient of liquid Fe. *Phys B: Condens Matter.* 2013;426:127–131.
- [20] Cao Q-L, Wang P-P, Huang D-H, et al. Transport coefficients and entropy-scaling law in liquid iron up to Earth-core pressures. *J Chem Phys.* 2014;140:114505(1)–114505(7).
- [21] Pasturel A, Jakse N. On the role of entropy in determining transport properties in metallic melts. *J Phys: Condens Matter.* 2015;27:325104(1)–325104(6).
- [22] Abramson EH. Viscosity of water measured to pressures of 6 GPa and temperatures of 300°C. *Phys Rev E.* 2007;76:051203(1)–051203(6).
- [23] Abramson EH, West-Foyle H. Viscosity of nitrogen measured to pressures of 7 GPa and temperatures of 573 K. *Phys Rev E.* 2008;77:041202(1)–041202(5).
- [24] Abramson EH. Viscosity of carbon dioxide measured to a pressure of 8 GPa and temperature of 673 K. *Phys Rev E.* 2009;80:021201(1)–021201(3).
- [25] Abramson EH. Viscosity of methane to 6 GPa and 673 K. *Phys Rev E.* 2011;84:062201(1)–062201(4).
- [26] Abramson EH. Viscosity of fluid nitrogen to pressures of 10 GPa. *J Phys Chem B.* 2014;118:11792–11796.
- [27] Belyukov AL, Ladyanov VI. An automated setup for determining the kinematic viscosity of metal melts. *Instrum Exp Tech.* 2008;51:304–310.
- [28] Khusnutdinoff RM, Mokshin AV, Menshikova SG, et al. Viscous and acoustic properties of AlCu melts. *J Exp Theor Phys.* 2016;122:859–868.
- [29] The oxide handbook, edited by Samsonov GV. 2nd ed. New York: Plenum; 1982.

- [30] Passianot R, Savino EJ. Embedded-atom-method interatomic potentials for hcp metals. *Phys Rev B*. 1992;45:12704–12710.
- [31] Belashchenko DK. Computer simulation of liquid metals. *Phys Usp*. 2013;56:1176–1216.
- [32] González LE, González DJ, López JM. Pseudopotentials for the calculation of dynamic properties of liquids. *J Phys: Condens Matter*. 2001;13:7801–7825.
- [33] Hansen JP, McDonald IR. *Theory of simple liquids*. New York: Academic Press; 2006.
- [34] Boon JP, Yip S. *Molecular hydrodynamics*. New York: McGraw-Hill; 1980.
- [35] Balucani U, Zoppi M. *Dynamics of the liquid state*. Oxford: Clarendon; 1994.
- [36] March NH. *Liquid metals: concepts and theory*. Cambridge: Cambridge University Press; 1990.
- [37] Forster D, Martin PC, Yip S. Moments of the momentum density correlation functions in simple liquids. *Phys Rev*. 1968;170:155–159.
- [38] Mokshin AV, Yulmetyev RM, Khusnutdinoff RM, et al. Collective dynamics in liquid aluminum near the melting temperature: theory and computer simulation. *J Exp Theor Phys*. 2006;103:841–849.
- [39] Mokshin AV, Yulmetyev RM, Khusnutdinoff RM, et al. Analysis of the dynamics of liquid aluminium: recurrent relation approach. *J Phys: Condens Matter*. 2007;19:046209(1)-046209(16).
- [40] Yulmetyev RM, Mokshin AV, Hänggi P. Diffusion time-scale invariance, randomization processes and memory effects in Lennard-Jones liquids. *Phys Rev E*. 2003;68:051201(1)-051201(5).
- [41] Khusnutdinoff RM, Mokshin AV. Vibrational features of water at the low-density/high-density liquid structural transformations. *Physica A*. 2012;391:2842–2847.
- [42] Rice SA, Kirkwood JG. On an approximate theory of transport in dense media. *J Chem Phys*. 1959;31:901–908.
- [43] Iida T, Guthrie RIL. *The thermophysical properties of metallic liquids. Vol. 1: fundamentals*. Oxford: Oxford Press; 2015.
- [44] Bodakin NE, Baum BA, Tyagunov GV. Viscosity of melts of the Fe-Co System. *Izv Vyssh uchebn zaved. Chern Metall*. 1978;7:9–13.
- [45] Frenkel J. *Kinetic theory of liquids*. New York: Dover; 1955.
- [46] Tankeshwar K, Pathak KN, Ranganathan S. The shear viscosity of Lennard-Jones fluids. *J Phys C: Solid State Phys*. 1988;21:3607–3617.
- [47] Adam G, Gibbs JH. On the temperature dependence of cooperative relaxation properties in glass-forming liquids. *J Chem Phys*. 1965;43:139–146.
- [48] Rosenfeld Y. Relation between the transport coefficients and the internal entropy of simple systems. *Phys Rev A*. 1977;15:2545–2549.
- [49] Rosenfeld Y. A quasi-universal scaling law for atomic transport in simple fluids. *J Phys: Condens Matter*. 1999;11:5415–5427.
- [50] Khusnutdinoff RM, Mokshin AV. Short-range structural transformations in water at high pressures. *J Non-Cryst Solids*. 2011;357:1677–1684.